Supporting Information

Evolutionary patterns of vane barb angles in birds

Xia Wang, Ho Kwan Tang and Julia A. Clarke

Included:

Dataset

Values for trailing vane angle and barb angle asymmetry for 25% feather length are significantly different for the Feo et al. sample. We chose to use the 50% values in this reanalysis since these were most similar to the measurement locations available for the majority fossil feathers sampled and because Feo et al. only provided 50% measurements for non-volant extant taxa. For Mesozoic taxa Measured values were compared to published values for specimens V15336, V13156, DNHM-D3078, BMNH-Ph000881 and Berlin specimen of *Archaeopteryx* utilized in that analysis.

Methods

(a) Phylogenetic signal and ancestral state reconstruction

Pagel's lambda [1] and Blomberg's K [2] were performed in R v. 3.0.1 [3] using the Phytools package (function phylosig [4]) to assess phylogenetic signal of barb angles. The influence of the phylogeny increases with lambda from 0 (no phylogenetic signal) and 1 (strong phylogenetic signal). When lambda = 0, a star phylogeny results with all tips radiating from a basal node, describing a model where traits evolve independent of the phylogeny. When lambda = 1, trait evolution followed a Brownian motion model, where branch lengths would be proportional to divergence. Blomberg's K statistic is used to test whether the observed distribution of traits exhibits more or less divergence than expected for traits evolving under Brownian motion. Values of K close to 1 indicate trait similarity is proportional to divergence and a Brownian motion model of evolution fits the data. K > 1 indicates that close relatives are more similar than expected, and K < 1 indicates more divergence between taxa than expected under a Brownian model.

Mesquite (v. 2.75 [5]) was used to map barb angles onto the reference phylogeny. Each character was traced onto the tree using the 'reconstruct ancestral state' module of Mesquite with weighted squared change parsimony [6]. Given the tree and observed character distribution, this method finds the ancestral states that minimize the number of steps of

character change.

1000 time-calibrated trees for the possible phylogenetic affinities of these 73 birds were sampled from the posterior distribution of Jetz et al [7] (http://www.birdtree.org). These trees use the Hackett et al [8] topology as a backbone. A majority rules consensus tree was built by Mesquite [5]. As taxa within passerines and rails are not fully resolved, the consensus tree was further resolved following recent phylogenetic hypotheses for passerines and rails [9, 10]. For Mesozoic taxa, we generate a fossil subtree with the timePaleoPhy function in paleotree [11] based on published fossil ages and branch [12, 13] (summarized in table S3). We grafted this time-calibrated tree of extinct taxa to the Aves tree with the bind.tip function in Phytools.

(b) Statistical analysis

All statistical analyses were conducted using the R statistical computing environment v.3.4.3 (R Development Core Team, 2017). To account for phylogeny via PGLS. ANOVA on PGLS models were conducted in R using the procD.pgls function in Geomorph package (residual randomisation permutation procedure) [14] and pairwise comparision was made in RRPP package [15]. The procD.pgls function performs ANOVA and regression models in a phylogenetic context under a Brownian motion model of evolution. The approach is derived from the statistical equivalency between parametric methods utilizing covariance matrices and methods based on distance matrices [14]. The randomization of residuals in a permutation procedure was used with1000 iterations. F statistics are calculated from sums of squares based on coefficients that have appropriately accounted for phylogenetic relatedness. Effect-sizes (Z scores) are computed as standard deviates of the F sampling distributions generated [14].

The function Phylogenetic generalized least-squares (pGLS) were also performed in R package Caper [16] to assess the relationship between trailing vane barb angle and barb angle asymmetry. We categorized flight styles for living birds as those defined by Bruderer et al [17]. Specifically, “continuous flapping”, “flapping and soaring”, “flapping and gliding” and “passerine type flight”. Flightless species and fossils were categoried as disticnt flight styles in this study. Measurements were log transformed to obtain a normal distribution as methods used have the assumption of normally distributed data.

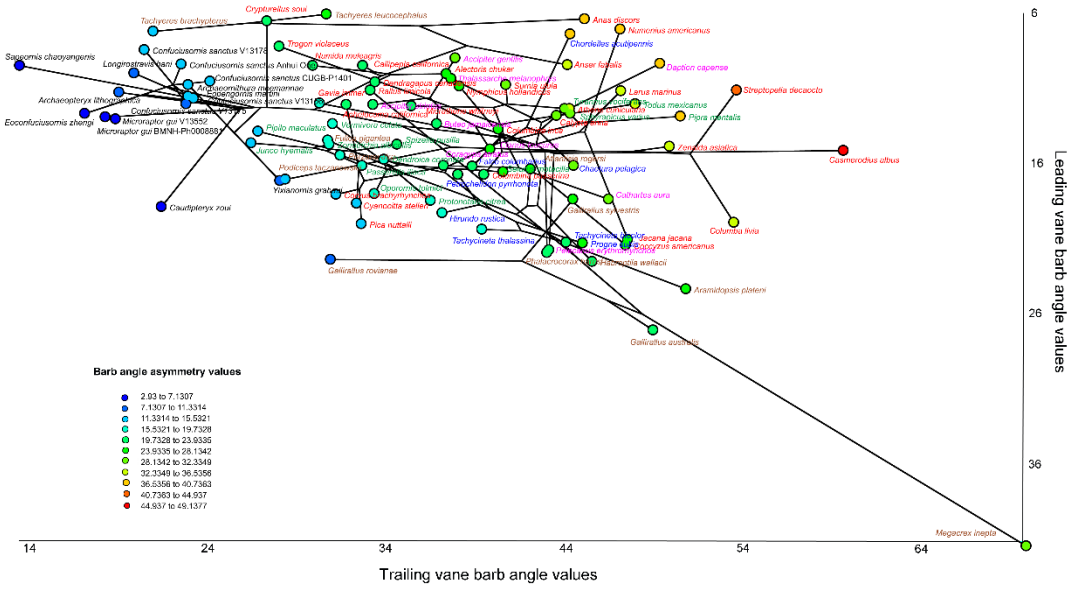

Figure S1. Aves with different flight styles and Mesozoic taxa plotted in a wing phylomorphospace described by leading and trailing vane barb angles. Red, continuous flapping “CF”; blue, flapping and soaring “FS”; purple, flapping and gliding “FG”; green, passerine type flight “PT”; brown, flightless “FL”; black, fossil data.

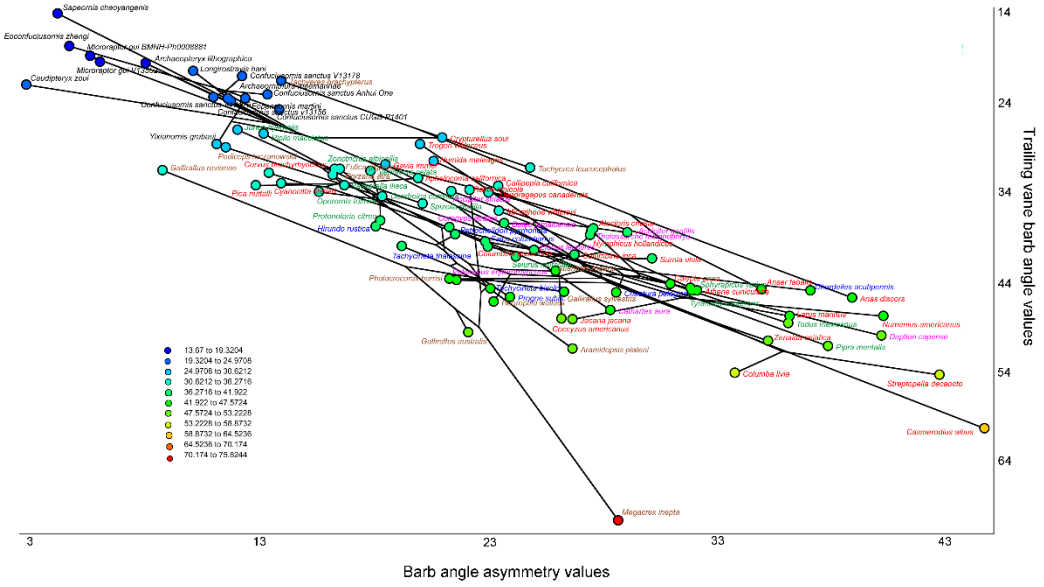

Figure S2. Aves with different flight styles and Mesozoic taxa plotted in a wing phylomorphospace described by trailing vane barb and barb angle asymmetry values. Red, continuous flapping “CF”; blue, flapping and soaring “FS”; purple, flapping and gliding “FG”; green, passerine type flight “PT”; brown, flightless “FL”; black, fossil data.

Interestingly, we found that distinct from other water birds, loons showed very reduced barb angles and angle asymmetry (11.829 and 30.508 for leading and trailing vane barb angles), similar to those of grebes (Figures 1,2, S2).

As barb angles were measured from different feathers and positions, we also mapped the values of barb angle variance across modern flight species. Similar patterns were recovered in ancestral state reconstructions of angle variance values. The leading vane and angle asymmetry values show reduced variance in galloanseres and passerines. Variance for trailing vane barb angles is also small in passerines (Figures S3-S5).

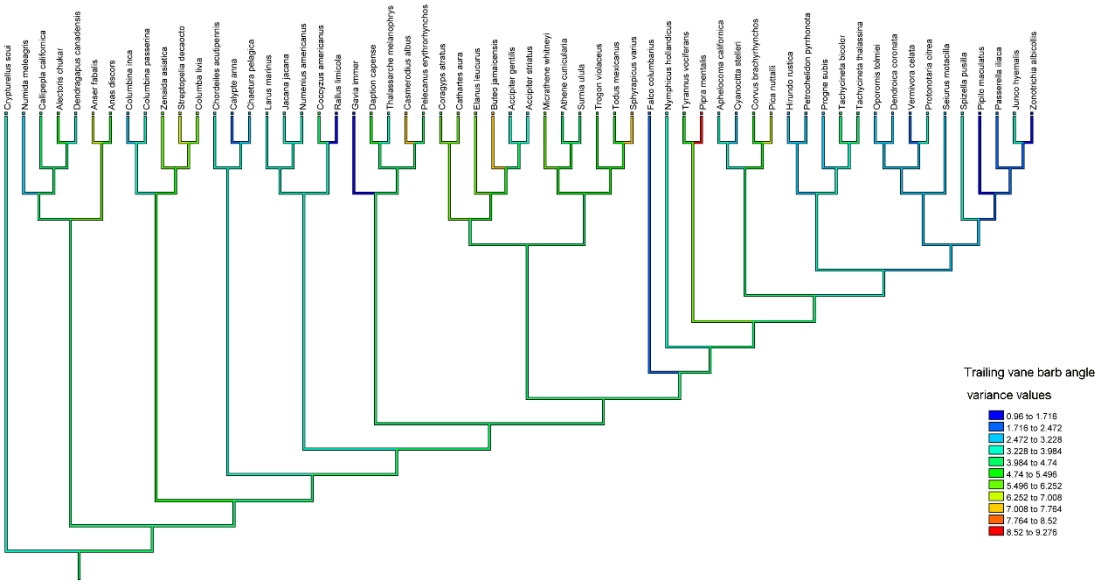

Fig S3. Changes in trailing vane barb angle variance from different feathers (inner, middle and outer) and positions (25% and 50% from feather tip) across extant flight species.

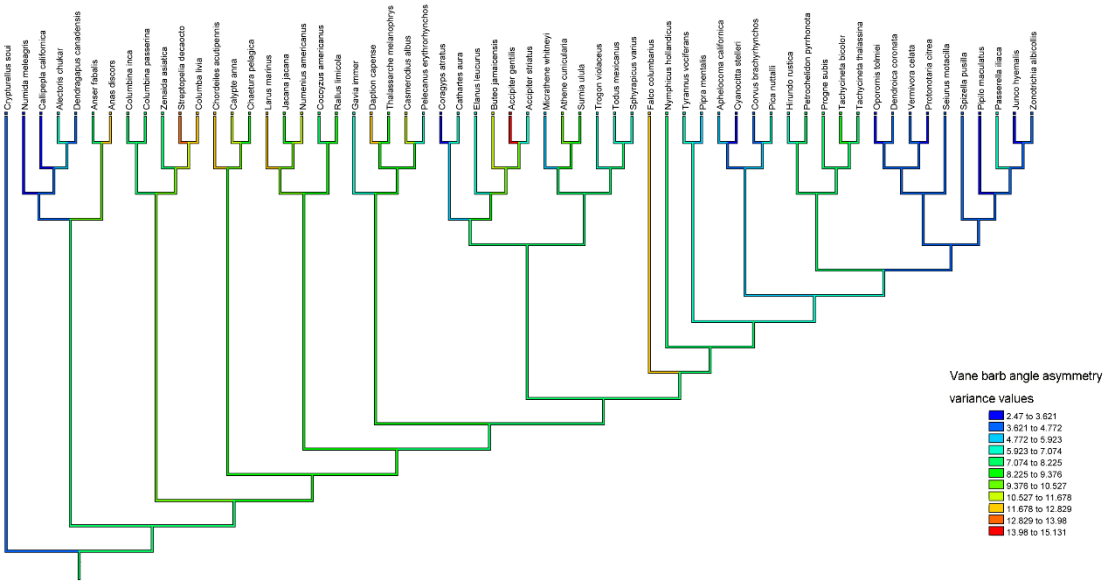

Fig. S4 Changes in vane barb angle asymmetry variance from different (inner, middle and outer) and positions (25% and 50% from feather tip) across extant flight species.

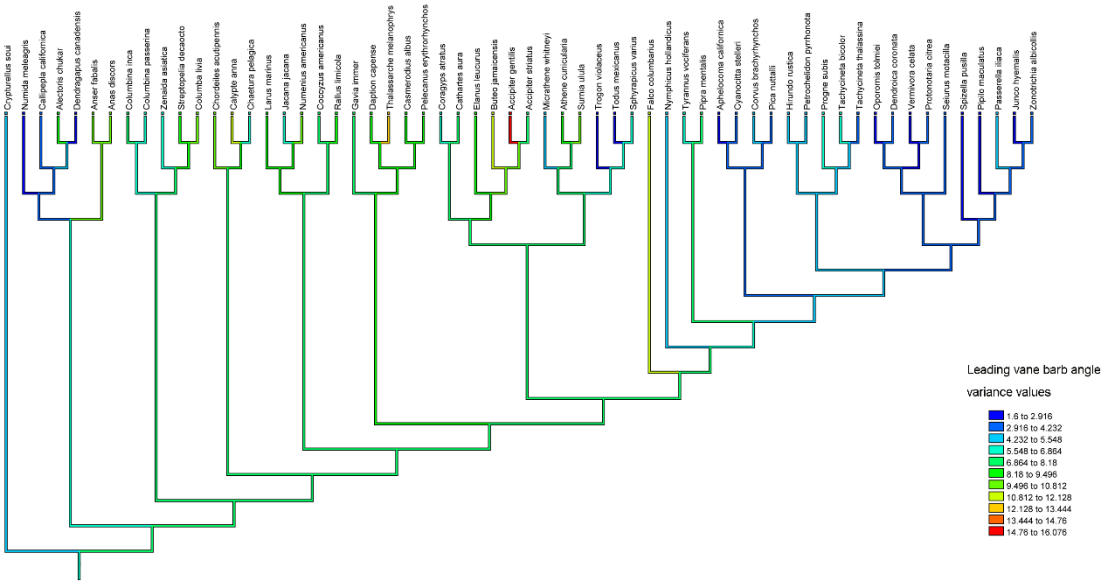

Fig. S5 Changes in Leading vane barb angle variance from different (inner, middle and outer) and positions (25% and 50% from feather tip) across extant flight species.

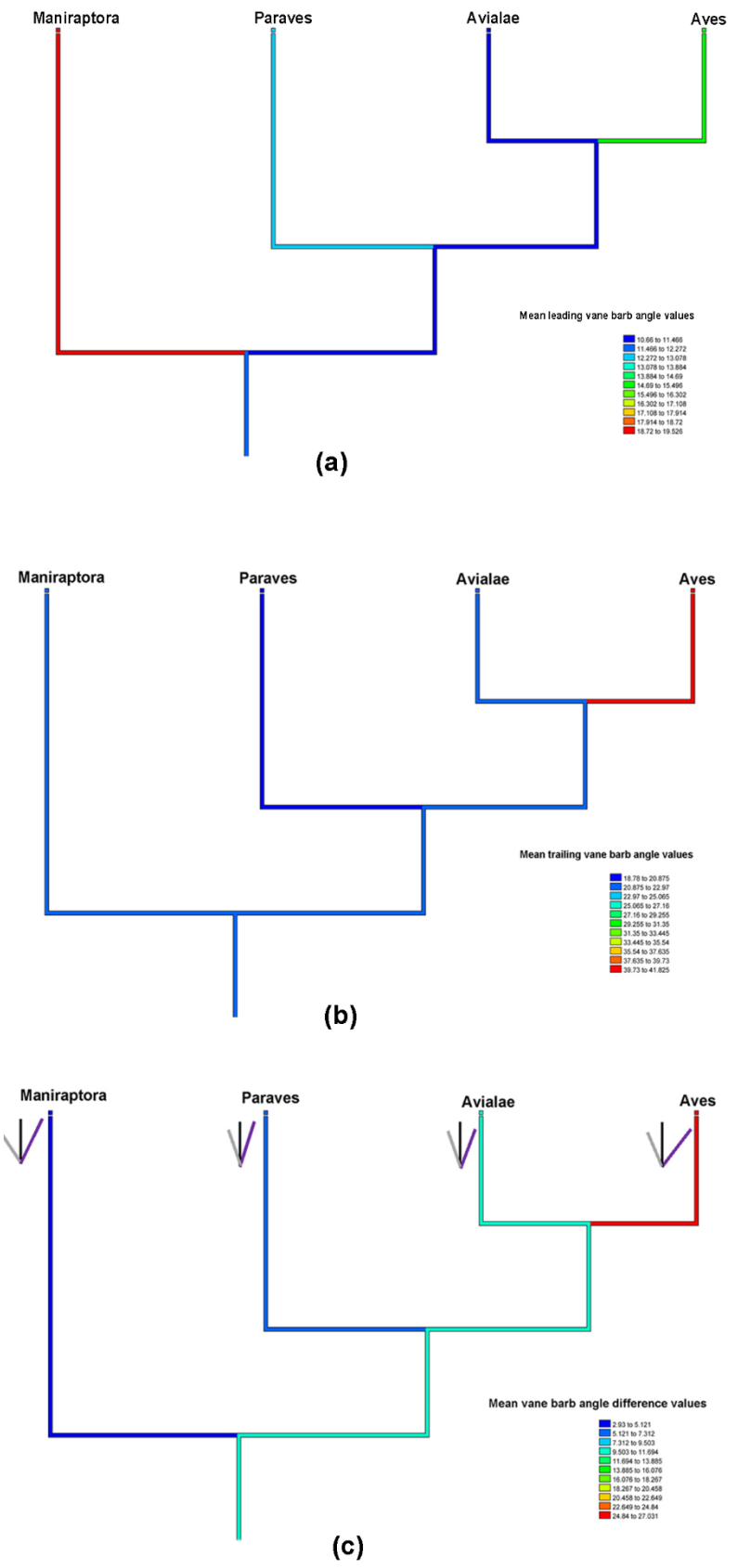

Fig. S6 Ancestral state reconstruction for leading (a), trailing (b) vane barb angles and barb angle asymmetry (c) showing the general evolutionary pattern for simplified phylogeny. Diagrams show the barb geometry. Grey, leading vane barb; purple, trailing vane barb.

Table S1. Measurements used for extant birds from Feo et al. (2015)*

Species	Ld	Tr	Diff	flight style
Coragyps_atratus	16.008	37.495	21.488	FS
Cathartes_aura	18.222	46.757	28.535	FS
Elanus_leucurus	14.887	40.099	25.212	FS
Buteo_jamaicensis	13.223	37.100	23.878	FS
Accipiter_gentilis	8.849	38.133	29.284	FS
Accipiter_striatus	11.916	33.505	21.589	FS
Anser_fabalis	9.269	44.457	35.187	CF
Anas_discors	6.226	45.384	39.158	CF
Tachyeres_brachypterus	7.067	21.171	14.104	FL
Tachyeres_leucocephalus	5.885	30.917	25.031	FL
Calypte_anna	12.664	43.836	31.172	CF
Chaetura_pelagica	15.973	44.779	28.806	FG
Chordeiles_acutipennis	7.250	44.577	37.327	FG
Jacana_jacana	20.919	47.810	26.891	CF
Numenius_americanus	6.903	47.417	40.514	CF
Larus_marinus	11.022	47.423	36.401	CF
Zenaida_asiatica	14.690	50.156	35.466	CF
Streptopelia_decaocto	10.968	53.943	42.975	CF
Columba_livia	19.787	53.782	33.996	CF
Columbina_inca	13.582	40.570	26.989	CF
Columbina_passerina	16.558	39.732	23.175	CF
Todus_mexicanus	11.874	48.230	36.356	PT
Coccyzus_americanus	21.291	47.710	26.419	CF
Falco_columbarius	16.050	39.114	23.064	FG
Callipepla_californica	9.340	32.963	23.623	CF
Alectoris_chukar	9.855	37.650	27.794	CF
Dendragapus_canadensis	10.427	33.645	23.218	CF
Numida_meleagris	9.331	30.138	20.807	CF
Gavia_immer	11.829	30.508	18.679	CF
Habroptila_wallacii	22.393	45.832	23.440	FL
Atlantisia_rogersi	16.218	42.375	26.156	FL
Fulica_gigantea	14.321	31.000	16.679	FL
Porzana_atra	15.295	31.664	16.369	FL
Aramidopsis_plateni	24.205	51.094	26.890	FL
Megacrex_inepta	41.273	70.174	28.901	FL
Gallirallus_australis	26.919	49.250	22.331	FL
Gallirallus_sylvestris	18.205	44.733	26.528	FL
Gallirallus_rovianae	22.229	31.150	8.921	FL
Rallus_limicola	10.985	33.354	22.369	CF
Tyrannus_vociferans	12.215	44.285	32.070	PT
Pipra_mentalis	12.715	50.799	38.085	PT
Aphelocoma_californica	11.925	32.040	20.115	CF
Cyanocitta_stelleri	18.498	32.615	14.118	CF
Corvus_brachyrhynchos	17.885	31.449	13.564	CF
Pica_nuttalli	19.881	32.875	12.995	CF
Hirundo_rustica	19.154	37.410	18.256	FG
Petrochelidon_pyrrhonota	16.564	38.299	21.736	FG
Progne_subis	21.154	45.293	24.139	FG

Tachycineta_bicolor	21.071	44.374	23.303	FG
Tachycineta_thalassina	20.222	39.624	19.402	FG
Oporornis_tolmiei	17.854	33.617	15.762	PT
Protonotaria_citrea	18.292	36.756	18.464	PT
Dendroica_coronata	15.581	34.123	18.542	PT
Seiurus_motacilla	16.396	40.809	24.414	PT
Vermivora_celata	13.224	31.267	18.043	PT
Junco_hyemalis	14.478	26.672	12.194	PT
Zonotrichia_albicollis	14.593	31.064	16.471	PT
Passerella_iliaca	16.000	32.891	16.891	PT
Pipilo_maculatus	13.719	27.074	13.354	PT
Spizella_pusilla	14.567	34.880	20.313	PT
Casmerodius_albus	14.982	59.920	44.937	CF
Pelecanus_erythrorhynchos	21.610	43.411	21.801	FS
Phalacrocorax_harrisi	21.789	43.270	21.481	FL
Sphyrapicus_varius	12.498	44.609	32.112	PT
Podiceps_taczanowskii	16.903	28.605	11.702	FL
Daption_capense	9.175	49.622	40.447	FS
Thalassarche_melanophrys	10.181	37.892	27.711	FS
Nymphicus_hollandicus	10.707	38.358	27.652	CF
Micrathene_whitneyi	12.011	35.665	23.655	CF
Athene_cunicularia	12.207	44.568	32.361	CF
Surnia_ulula	10.595	40.984	30.389	CF
Crypturellus_soui	6.378	27.558	21.180	CF
Trogon_violaceus	8.041	28.254	20.213	CF

Ld, leading vane angle; Tr, trailing vane angle; Diff, barb angle differences; CF, continours flapping; FS, flapping and soaring; FG, flapping and gliding; PT, passerine type flight; FL, flightless
*Specimen numbers and localities can be found from Feo et al. (2015).

Table S2 Measurements used for fossil taxa

Specimen No.	Species	Ld	Tr	Diff
STM-7-145	*Archaeornithura meemannae*	10.62	23.16	12.54
V13631	*Yixianornis grabaui*	17.00	28.29	11.29
V11309	*Longirostravis hani*	9.85	20.12	10.27
STM-24-1	*Eopengornis martini*	7.42	23.59	16.16
V15336	*Eopengornis martini*	11.13	19.46	8.33
V13156	*Confuciusornis sanctus*	11.37	23.14	11.77
CUGB-P1401	*Confuciusornis sanctus*	10.36	24.38	14.03
AGB5488	*Confuciusornis sanctus*	9.22	22.75	13.53
V13178	*Confuciusornis sanctus*	8.27	20.69	12.41
V13175	*Confuciusornis sanctus*	11.87	23.02	11.15
V11977	*Eoconfuciusornis zhengi*	12.50	17.34	4.84
DNHM-D3078	*Sapeornis chaoyangensis*	7.84	13.78	5.93
Berlin specimen	*Archaeopteryx lithographica*	11.11	19.27	8.17
BMNH-Ph000881	*Microraptor gui*	12.74	18.48	5.74
V13352	*Microraptor gui*	12.90	19.08	6.18
NGMC 97-4-A DSC2551	*Caudipteryx zoui*	18.72	21.66	2.93

Ld, leading vane angle; Tr, trailing vane angle; Diff, barb angle differences; STM, Shandong Tianyu Natural History Museum; V, Institute of Vertebrate Paleontology and Paleoanthropology; CUGB, China University of Geosciences (Beijing); DNHM, Dalian Natural History Museum; BMNH, Beijing Museum of Natural History; NGMC, National Geological Museum of China.

Table S3 Fossil age (Ma) data for paleotree [31].

Species	Min_age	Max_age	Start	End	Midpoint
Yixianornis_grabaui	Aptian	Aptian	126.3	113	119.65
Longirostravis_hani	Late_Barremian	Early_Aptian	128.55	119.65	124.1
Eopengornis_martini	Hauterivian	Hauterivian	133.9	130.8	132.35
Confuciusornis_sanctus	Late_Barremian	Early_Aptian	128.55	119.65	124.1
Eoconfuciusornis_zhengi	Hauterivian	Hauterivian	133.9	130.8	132.35
Sapeornis_chaoyangenis	Aptian	Aptian	126.3	113	119.65
Archaeopteryx_lithographica	Early_Tithonian	Early_Tithonian	152.1	147.7	149.9
Microraptor_gui	Aptian	Aptian	126.3	113	119.65
Caudipteryx_zoui	Aptian	Aptian	126.3	113	119.65
Archaeornithura_meemannae	Hauterivian	Hauterivian	133.9	130.8	132.35

10. Images showing the angle measurements of Mesozoic fossil taxa.

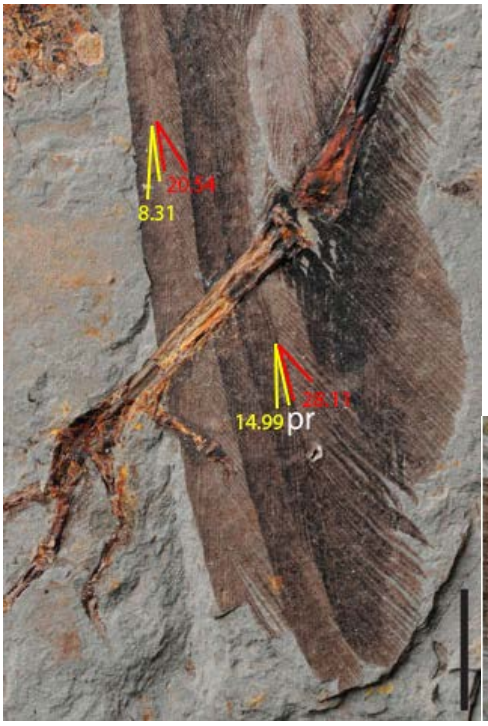

Archaeornithura meemannae (STM7-145)

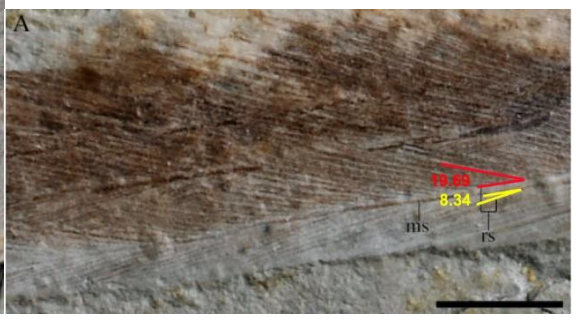

Eopengornis martini (V15336)

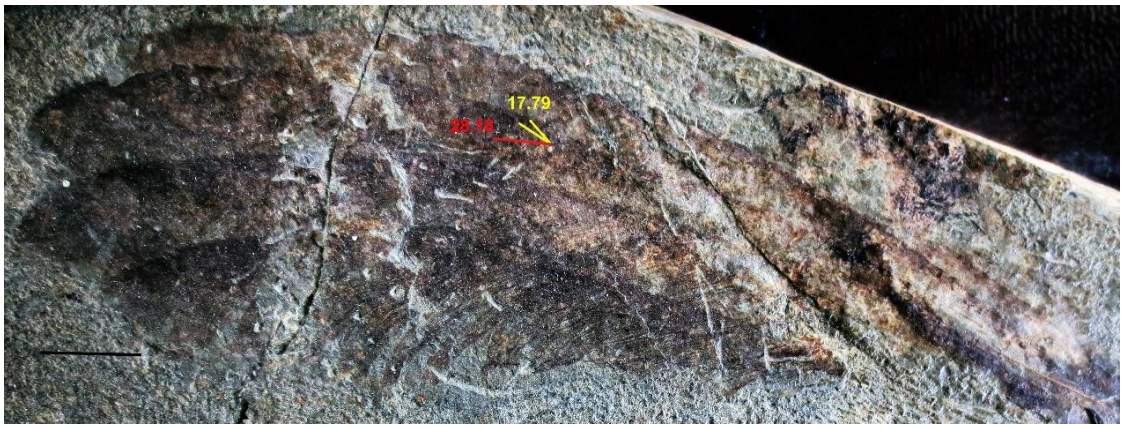

Yixianornis grabaui (V13631)

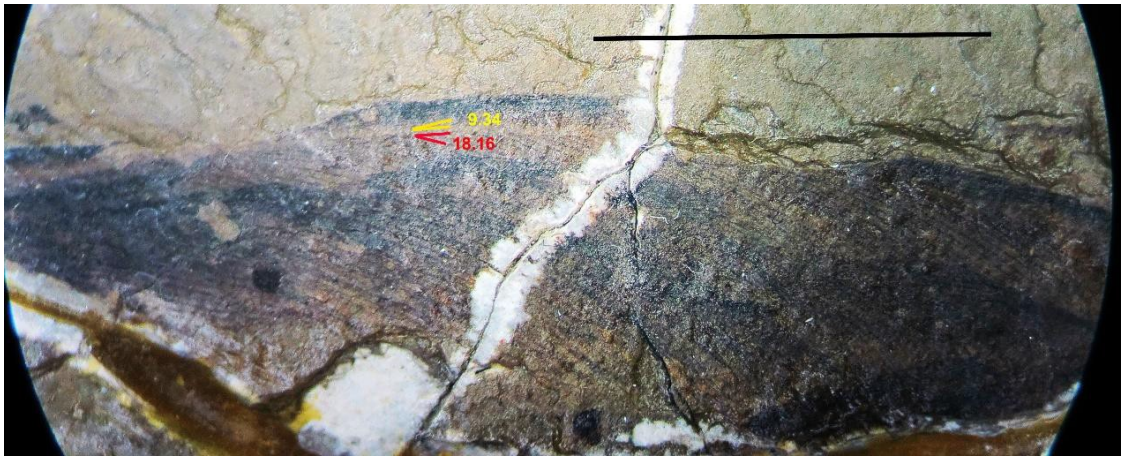

Longirostravis hani (V11309)

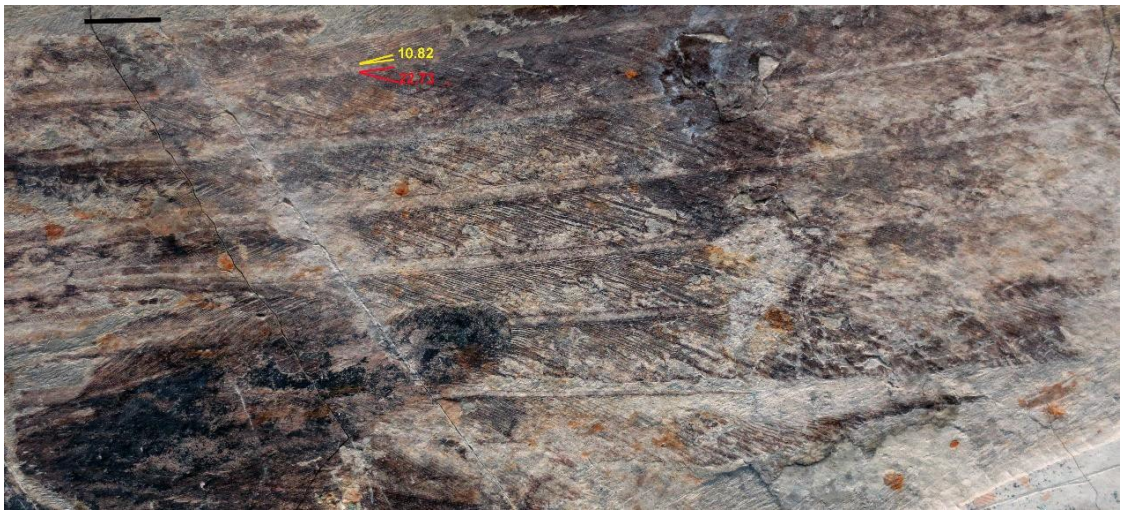

Confuciusornis sanctus(V13156)

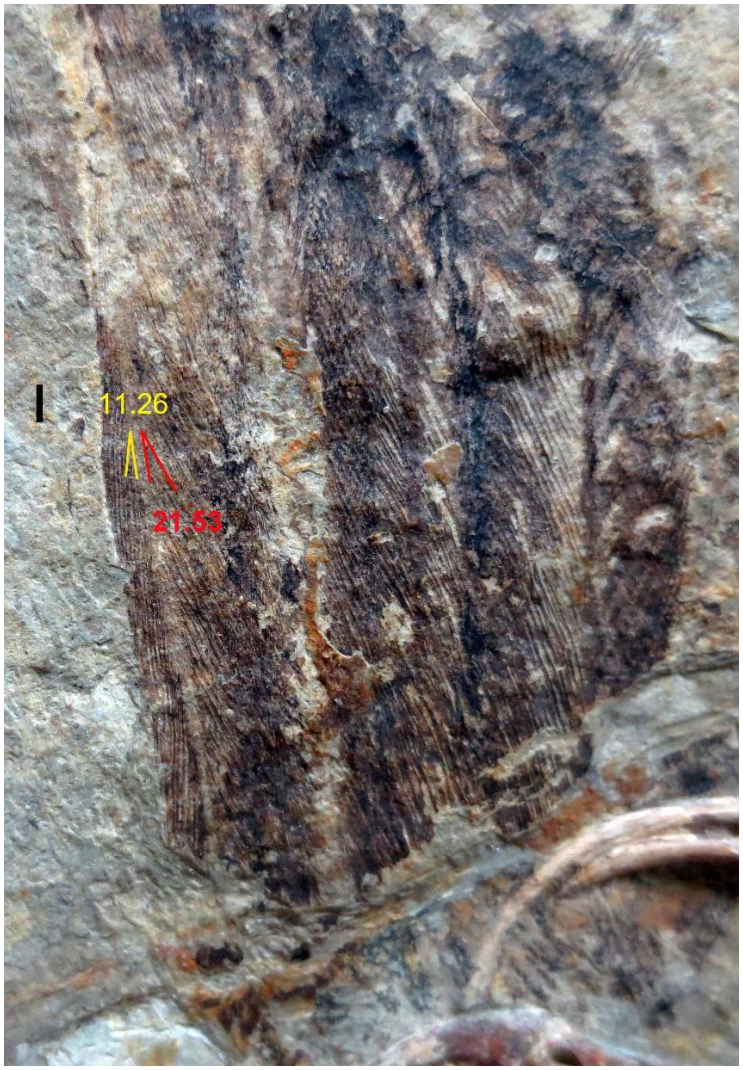

Confuciusornis sanctus (V13175)

Confuciusornis sanctus (V13178a)

***Confuciusornis sanctus* (V13178b)**

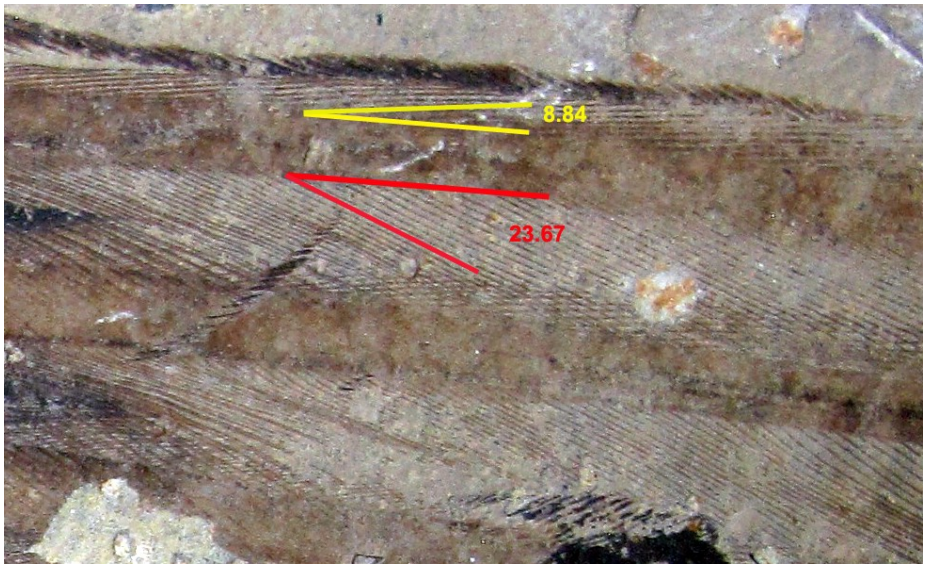

***Confuciusornis sanctus* (AGB5488)**

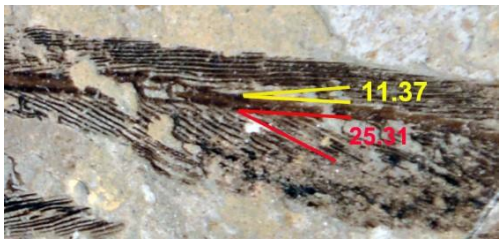

Confuciusornis sanctus **(CUGB-P1401)**

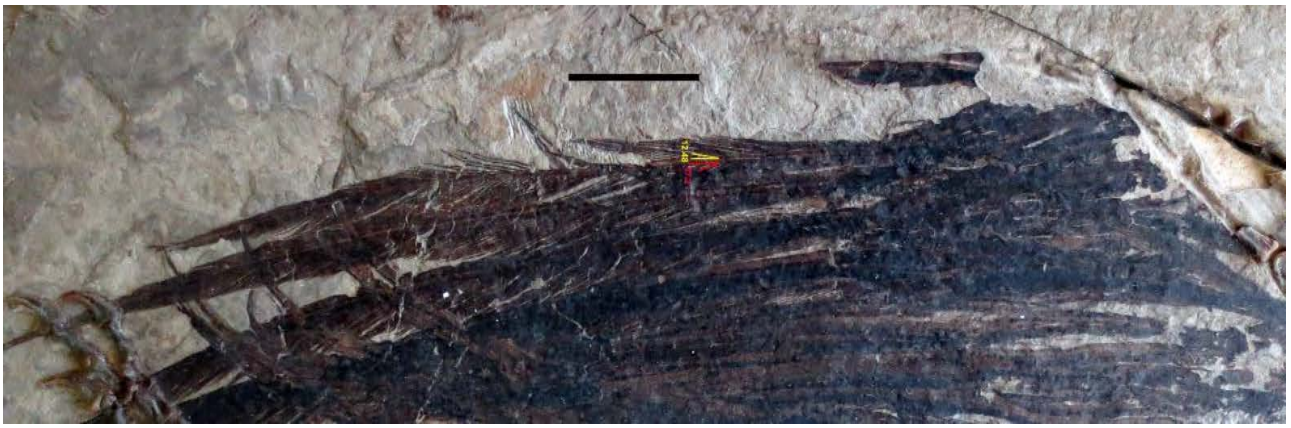

Eoconfuciusornis zhengi **(V11977)**

Sapeornis chaoyangensis **(DNHM-D3078)**

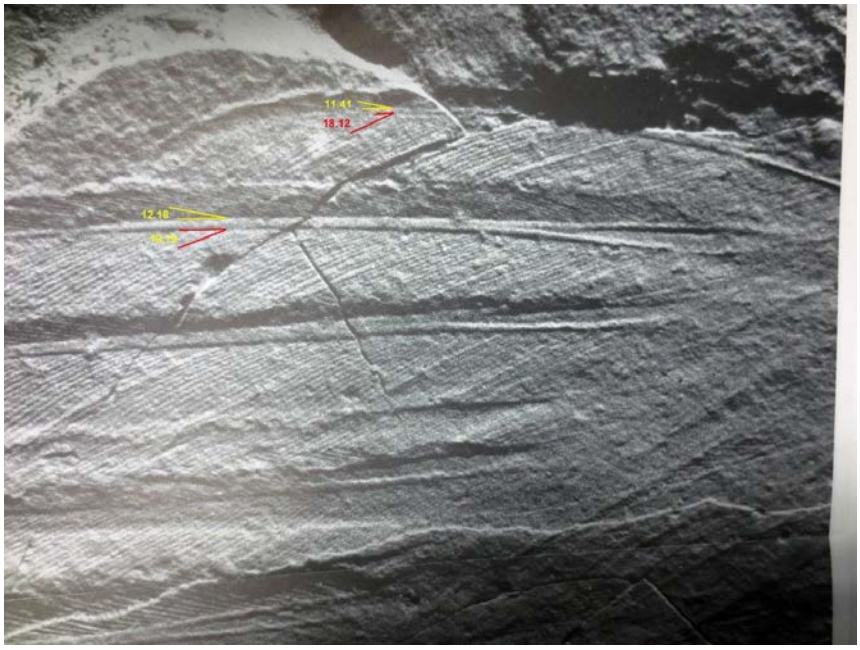

Archaeopteryx lithographica **(Berlin specimen)**

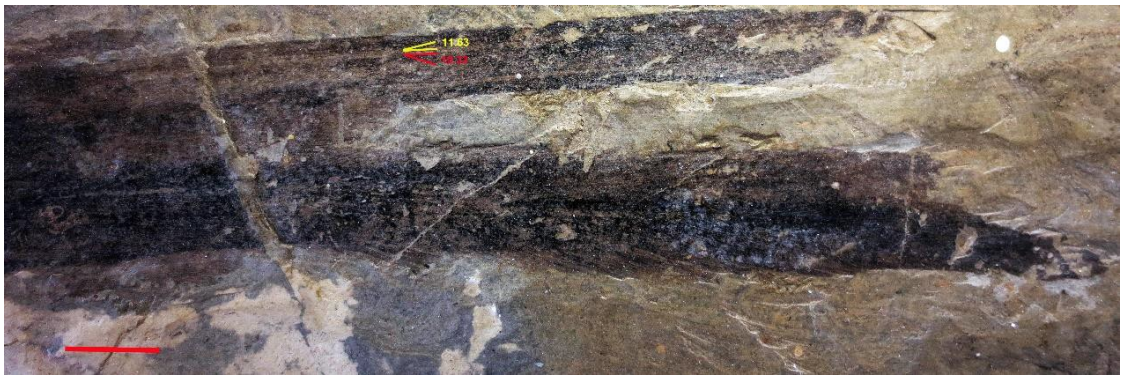

Microraptor gui **(V13352)**

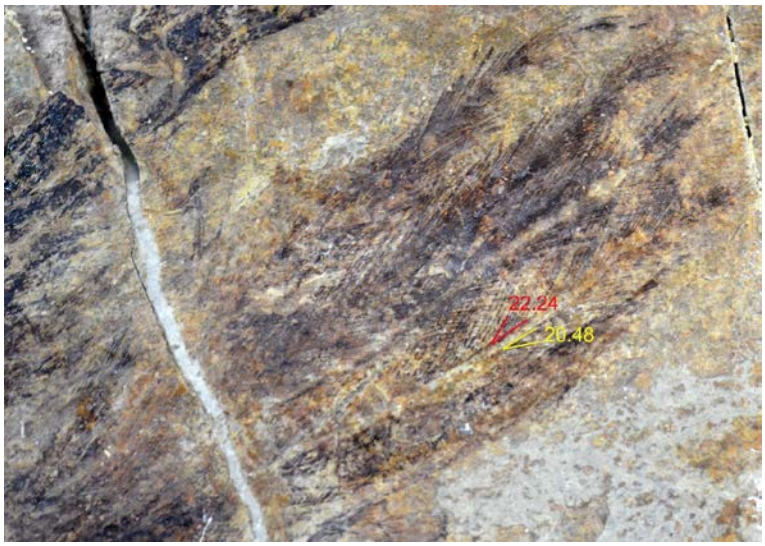

Caudipteryx zoui **(NGMC 97-4-A DSC2551)**

1. Pagel M. 1999 Inferring the historical patterns of biological evolution. *Nature* **401**, 877-884.
2. Blomberg SP, Garland TIves AR. 2003 Testing for phylogenetic signal in comparative data: behavioral traits are more labile. *Evolution* **57**, 717-745.
3. Team R. 2013 R Development Core Team.
4. Revell LJ. 2012 phytools: an R package for phylogenetic comparative biology (and other things). *Methods Ecol. Evol.* **3**, 217-223.
5. Maddison W, Maddison D. 2011 Mesquite 2.75: a modular system for evolutionary analysis. https://www.mesquiteproject.org
6. Maddison DR. 1991 The discovery and importance of multiple islands of most-parsimonious trees. *Systematic Biol.* **40**, 315-328.
7. Jetz W, Thomas G, Joy J, Hartmann K, Mooers A. 2012 The global diversity of birds in space and time. *Nature* **491**, 444-448.
8. Hackett SJ, Kimball RT, Reddy S, Bowie RC, Braun EL, Braun MJ, Chojnowski JL, Cox WA, Han K-L, Harshman J. 2008 A phylogenomic study of birds reveals their evolutionary history. *Science* **320**, 1763-1768.
9. Barker FK, Burns KJ, Klicka J, Lanyon SM, Lovette IJ. 2015 New insights into New World biogeography: An integrated view from the phylogeny of blackbirds, cardinals, sparrows, tanagers, warblers, and allies. *Auk* **132**, 333-348.
10. Garciar JC, Gibb GC, Trewick SA. 2014 Deep global evolutionary radiation in birds: diversification and trait evolution in the cosmopolitan bird family Rallidae. *Mol. Phylogenet. Evol.* **81**, 96-108.
11. Bapst DW. 2012 paleotree: an R package for paleontological and phylogenetic analyses of evolution. *Methods Ecol. Evol.* **3**, 803-807.
12. Clarke J. 2013 Feathers Before Flight. *Science* **340**, 690-692. (doi:10.1126/science.1235463).
13. Eliason CM, Clarke JA. 2018 Metabolic physiology explains macroevolutionary trends in the melanic colour system across amniotes. *Proc. R. Soc. B.* **285**, 20182014.
14. Adams DC, Collyer M, Kaliontzopoulou ASherratt E. 2016 Geomorph: Software for geometric morphometric analyses.
15. Collyer M, Adams DC. 2018 RRPP: An r package for fitting linear models to high-dimensional data using residual randomization. *Methods Ecol. Evol.* **9**, 1772-1779.
16. Orme D, Freckleton R, Thomas G, Petzoldt T, Fritz S, Isaac N, Pearse W. 2012 Caper: comparative analyses of phylogenetics and evolution in R. R package version 0.5.
17. Bruderer B, Peter D, Boldt A, Liechti F. 2010 Wing-beat characteristics of birds recorded with tracking radar and cine camera. *Ibis* **152**, 272-291.